Optimization of Beam Configurations for Shock Ignition Experiments on the NIF and OMEGA

Patricia Olson

Brighton High School

Rochester, New York

Adviser: Dr. R. S. Craxton

Laboratory for Laser Energetics

University of Rochester

Rochester, New York

November 2011

1. Abstract

Beam configurations were optimized for shock ignition experiments at both the National Ignition Facility (NIF) and the OMEGA Laser Facility. Shock ignition involves two different laser pulses, one to compress the target, and the other to ignite it. On the NIF, to compensate for the configuration of the laser quads, the beams are repointed towards the equator of the target in a method known as polar drive. The NIF experiment uses 96 out of 192 beams for the compression pulse, and the other 96 for the ignition pulse. The compression beams were optimized to provide a deviation of 3.5 microns, or 0.74% rms in the center of mass radius after implosion through 465 microns. The pointings used for the compression beams can be remapped and scaled to be used for the shock beams. The OMEGA experiment delivers the compression pulse to 40 of the 60 beams, and the shock pulse to the other 20. Adjustments to the compression beams led to an energy deposition uniformity of 1.2% rms, while adjustments to the shock beams resulted in uniformity of 3.9% rms. These results were achieved by running numerous 2-D hydrodynamic simulations using the code *SAGE* in which various parameters were adjusted.

2. Introduction

Nuclear fusion is a possible source for clean, renewable energy. One approach for achieving nuclear fusion is to irradiate a small spherical target made of a glass or plastic shell filled with deuterium and tritium, isotopes of hydrogen, with high power lasers.[1] The outside of the shell ablates outward while the inner part of the shell implodes, compressing the deuterium and tritium gas and causing it to reach an extremely high temperature and pressure. The high temperature of the gas allows the positively charged nuclei to overcome their repulsion forces, and the high pressure ensures a large number of fusion reactions before the target explodes. The deuterium and tritium nuclei fuse to create a helium nucleus and a high energy neutron. These energetic neutrons comprise most of the energy

2

released by the fusion reactions. If the product of the density of the fuel and the radius of the target is great enough, the energy of the helium nucleus will be deposited in the fuel. This is known as ignition. When ignition occurs, the energy released by the fusion reactions will be greater than the energy input by the lasers, an event known as breakeven. Laser fusion will be useful as an energy source once high energy gain is achieved: when the energy produced is one hundred times the energy put in.
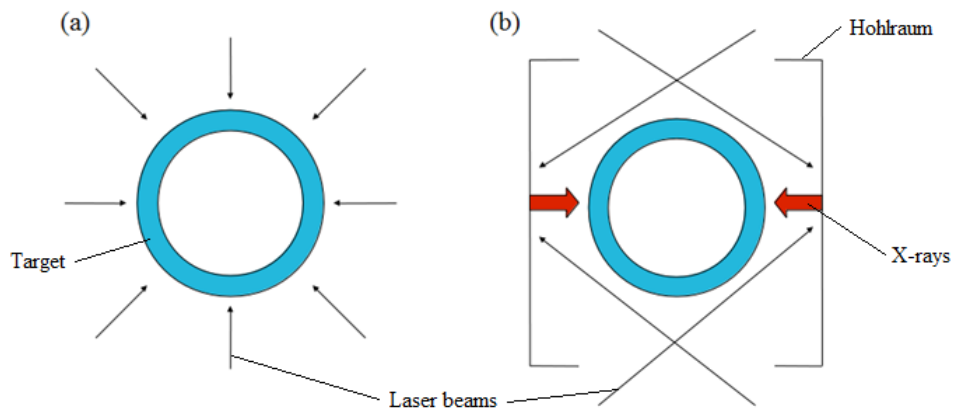

Figure 1: The two main approaches to inertial confinement fusion. (a) Direct drive involves pointing laser beams directly at the target in order to irradiate it. (b) Indirect drive involves pointing the laser beams at the inside of a cylindrical hohlraum, generating X-rays which irradiate the target.

There are two different approaches to laser fusion: direct drive and indirect drive. Direct drive involves pointing laser beams located all around the target at the center of the target so that they hit it at normal incidence [Figure 1(a)]. This is the approach for which the Laboratory for Laser Energetics OMEGA laser is configured. High uniformity is very important to achieving high compression and therefore high energy yields. In indirect drive, the target is surrounded by a hohlraum, a metal cylinder made of gold or another heavy metal [Figure 1(b)]. The laser beams are aimed at the inner walls of the hohlraum, entering through holes at the top and bottom. When the laser beams strike the inside of the hohlraum, they create X-rays which then irradiate the target, compressing it. Nearly all the initial energy from the laser beams is absorbed by the metal of the hohlraum, and nearly 80% is emitted in the

form of X-rays, but only 20% is absorbed by the target. The rest of the energy is lost as the X-rays are absorbed by the walls of the hohlraum or pass through the openings in the top and bottom. Though this method of laser fusion is far less efficient, it may result in more uniform irradiation of the target than is possible in direct drive. The National Ignition Facility (NIF) located at the Lawrence Livermore National Laboratory is configured for indirect drive. The NIF is currently the most powerful laser in the world. It has 192 beams divided into 48 quads, or sets of four beams, that deliver a total energy of 1.8 MJ to the target.
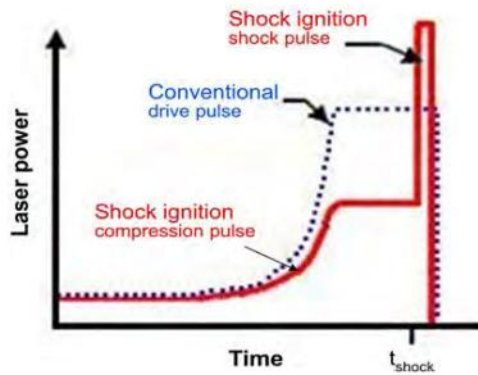

Figure 2: Graph comparing a conventional drive pulse and the compression and shock pulses of shock ignition. The dotted line depicts the conventional drive pulse, while the solid line shows the initial compression pulse and the final high power shock pulse.

Shock ignition is a concept for achieving maximum energy gain fusion. Traditional direct drive fusion experiments use a single long, high-intensity laser pulse which simultaneously compresses and ignites the fuel. Shock ignition splits the laser beams into two sets to deliver two pulses, which compress and ignite the fuel in two steps.[2] The first set delivers the compression pulse: a low intensity, long pulse used to compress the target as much as possible. This allows a greater mass of fuel to be compressed without having to reach the high temperature required for ignition. The second set of laser beams delivers the shock pulse: a short, high intensity pulse designed to achieve ignition. Figure 2 compares a traditional drive pulse to the shock pulse design. Experiments on both the NIF and OMEGA are planned to implement shock ignition.

OMEGA has a total of sixty beams which are positioned so that they form the vertices of a

4

truncated icosahedron. These beams originate from a single beam which is split into three beams, each of which is each split into twenty beams, adding up to the total of sixty beams. It is possible to put a separate pulse into one of the original three beams, creating twenty beams with one pulse shape and forty with another. This makes shock ignition experiments possible. A compression pulse can be delivered by forty of the sixty beams, and the other twenty can be used to deliver a shock pulse, but the sets of forty and twenty beams are not spaced uniformly around the target. If either set of beams were pointed at normal incidence at the target, energy deposition would be extremely non-uniform. The same problem occurs on the NIF, where it is desired to use half the beams for the compression pulse and half for the shock pulse. This is only compounded by the lack of beams at the equator of the target.

The goal of this work was to produce experimental designs for beam orientations to be used in experiments to be performed on both the NIF and OMEGA laser systems. Laser beams were shifted horizontally and vertically to optimize uniformity of energy deposition over the target surface. Optimized designs with high uniformities have been found for both systems that should allow for high energy yields.

3. Experimental Design for the NIF

There are 192 laser beams on the NIF, and laser beam ports are arranged in eight rings around the target, with four rings at angles of 23.5°, 30.0°, 44.5°, and 50.0° from vertical in both the upper and lower hemispheres. These angles allow the beams to hit the inside of the hohlraum at ideal angles. The beams are arranged such that there is a four-fold symmetry azimuthally. Laser beams are arranged in groups of four called quads. There are 48 quads, each occupying a single port in the target chamber. Each beam measures 35 cm by 35 cm square. The NIF was designed with another ring of ports at 77.45° from vertical in each hemisphere for possible future direct drive experiments, but reconfiguring

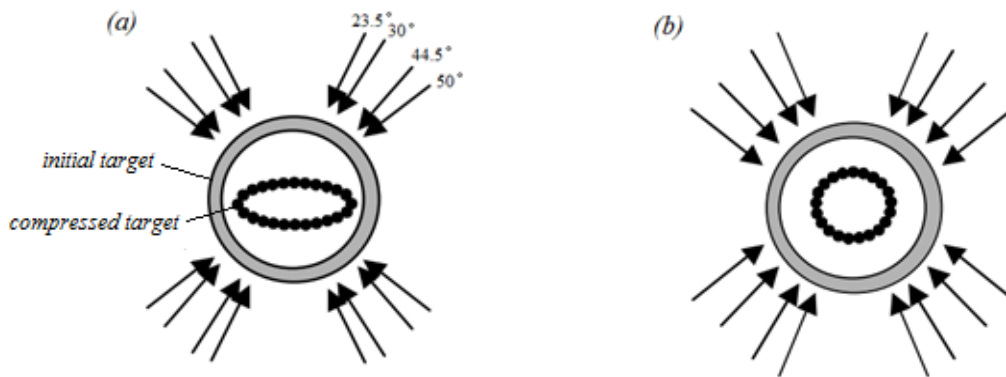the laser beams to these ports would be very expensive and time consuming.

Figure 3: Drive without repointings versus polar drive on the NIF. (a) Pointing the laser beams directly at the center of the target results in very low uniformity of the compressed target. (b) Using polar drive, shifting the beams towards the equator allows for maximum implosion uniformity.

In order to begin direct drive experiments on the NIF as soon as possible, the method of polar drive is being developed. Polar drive was proven to be a viable technique on OMEGA,[3] and it has been explored theoretically for the NIF.[4,5] If the beams are merely aimed at the center of the target, the target will receive much more drive on the poles than at the equator [Figure 3(a)]. The shell velocity at the poles in this scenario would be approximately three times as large as the shell velocity at the equator.[6] If the beams are repositioned towards the equator the target will be driven much more uniformly, and direct drive experiments become possible on the NIF [Figure 3(b)].

Design limitations on the NIF mean that it is impossible to deliver the compression and shock pulses from beams in the same quad. Therefore, quads must be split so that each quad only carries one pulse or the other. In the designs reported in this paper, half of the quads deliver the compression pulse, while the rest are reserved to deliver the shock pulse. Parameters were adjusted in order to achieve maximum uniformity in compression of the target.

The experiment on the NIF implements the two step shock ignition process using polar drive.

Since only half of the quads are to be used for each pulse, not only must the beams be repositioned towards the equator to compensate for the lack of beams in that location, but they must be adjusted azimuthally to compensate for the lower number of beams available to irradiate the target.

Tucker[7] developed an experimental design for the compression beams. Using the two-dimensional hydrodynamics code *SAGE*,[8] she optimized beam pointings azimuthally and in the polar direction, and adjusted other parameters described in Section 3.1 below. Her design, seen in Figure 4, has a uniformity of 1.81% (8.1 microns) rms in center of mass radius after implosion through 465 microns. The goal of this work was to improve upon Tucker's design by continuing to adjust these parameters, taking advantage of increased freedom allowed in development of the experimental design.

The variation in radius of the target from the average radius using Tucker's design can be seen in the profile in Figure 4. Shaded quads represent the locations of the quads used for the compression pulse, while the quads that are not filled in represent the locations of the quads that will eventually be used for the shock pulse. The areas of high and low compression over the target surface follow a clear pattern. Areas of high compression, represented by a gradient from yellow to red, occur mostly in areas close to the quads used for the compression pulse. Areas of low compression, represented by a gradient from green to blue, occur mostly in areas without quads used for the compression pulse. This design is a great improvement over a design with center pointed beams, but it still has areas of non-uniformity, especially near the equator. There is a clear repeating pattern of high and low compression areas on either side of the equator.
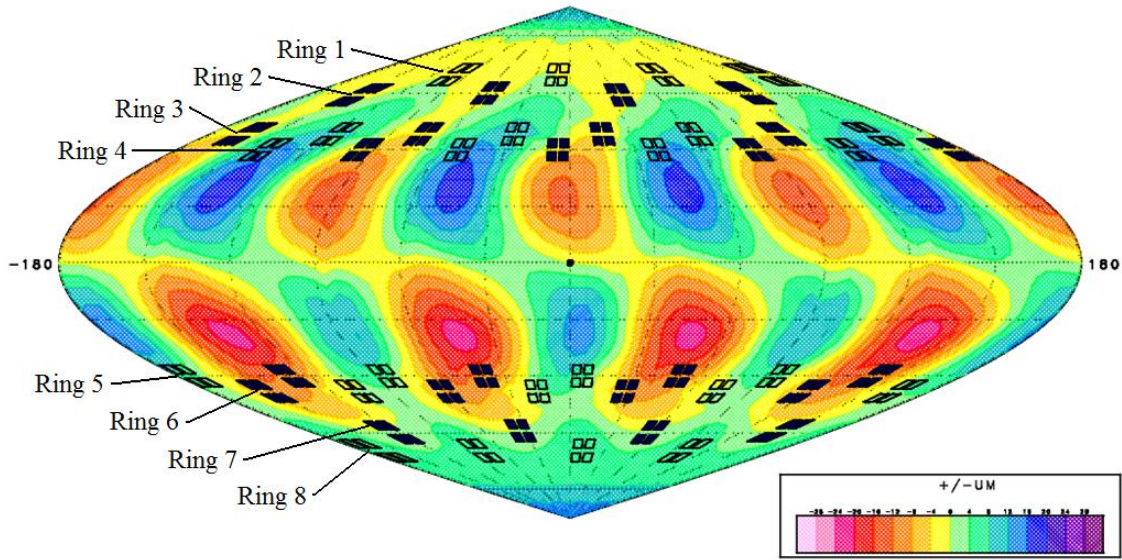
Figure 4: 3-D center of mass profile depicting non-uniformity over the target surface at 4 ns in Tucker's design (Ref. 7). Yellow and red areas represent the locations on the target shell that have a lower than average center of mass radius, while the green and blue areas depict locations with higher than average center of mass radius. The filled in quads represent the beams that are used for the compression pulse. This design had an rms of 1.81%. Beam rings are labeled in the top hemisphere.

3.1. Parameters for Optimization

In order to provide maximum uniformity in target compression, a number of parameters had to

be adjusted. Figure 5 shows the optics in the laser system that control beam shift and defocus.   Beams

are shifted by moving the mirror that reflects the laser beam onto the target. The beam moves a

specified distance perpendicular to its axis to cause the center of the beam to hit the target at a different

location. Beam spots are defocused by moving the focus lens towards the target. The beam spot on the

target increases in size and the maximum intensity decreases. The defocus of the beams must be

changed to allow beams to overlap and irradiate the target as uniformly as possible. It is also a way to

adjust the relative intensities of the four rings of beams. Indirect drive phase plates, optics used to

determine the best-focus laser beam spot size, can be used for polar drive experiments because of

defocusing.[8] The defocus increases the size of the beam spots enough that they are suitable for direct

8

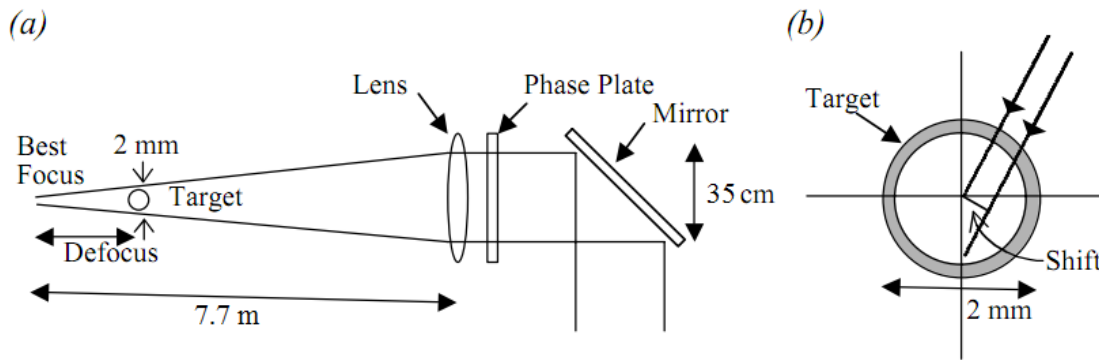drive despite the smaller size of the indirect drive beam spots.[9]

Figure 5: (a) Diagram (not to scale) depicting the components of the NIF laser involved in this work. (b) Diagram showing how beam shifts are measured perpendicular to the direction of the beam. This diagram depicts how a vertical shift is measured. [Ref. 9]

There were twelve different sets of beams in each hemisphere that could be shifted individually in the simulations. Each set of beams contained either four or eight beams spaced around the target surface in a ring. Rings are labeled in Figure 4. In the top hemisphere, there are two sets of beams in Rings 1 and 2 labeled from top to bottom: 1A, 1B, 2A, and 2B. Only beam sets 2A and 2B were used for the compression pulse, and all eight beams in each set were used. In the bottom hemisphere, sets 8A and 8B, corresponding to sets 1A and 1B in the top hemisphere, were used for the compression pulse. The top two beams in each quad (set 2A) could be moved the same amount vertically and horizontally, and the bottom two beams in each quad (set 2B) could be moved the same way. It was possible to choose whether to give each beam pair the same horizontal shift or opposite horizontal shifts [Figure 6]. The optimized design had all beams in set 2A moved one way and all beams in set 2B moved the other way, and included the same shifts in sets 8A and 8B in the bottom hemisphere.
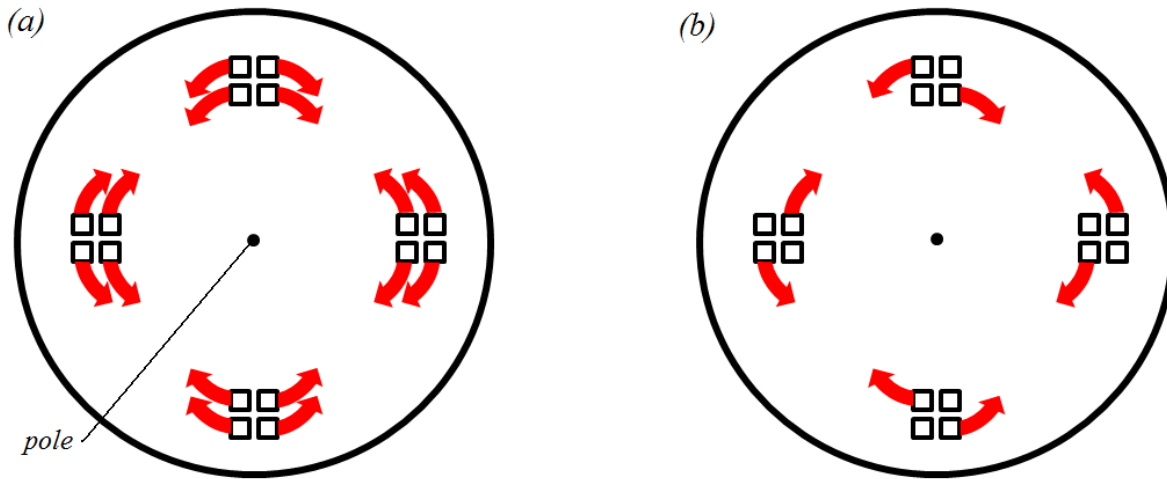
Figure 6: Depiction of two options for beam movement in Ring 2. Beam set 2A comprised of the inner eight beams in each diagram, and beam set 2B is comprised of the outer eight beams. (a) In the first option, beam pairs were moved with opposing horizontal shifts to spread out beam energy. (b) In the second option (and in the optimized design), beam pairs were given the same horizontal shift, but the inner pair was moved clockwise while the outer pair was moved counterclockwise.

There were four sets of beams in Rings 3 and 4, labeled 3A, 3B, 3C, 3D, 4A, 4B, 4C, and 4D. These beam sets can be seen in Figure 7. Each beam in a quad could be moved individually. This freedom was allowed by changes made to the *SAGE* code after Tucker's work. Tucker had the level of freedom shown in Figure 6(a) for every ring of beams. When shifts were given to these pairs of beams, they would always have the same vertical shift and opposite horizontal shifts. Energy from two different beams would often be deposited in the same location, as seen with sets 4B and 3C in Figure 7(a). This explains the pattern of high and low center of mass radii seen around the equator in Tucker's design [Figure 4]. In the optimized design, beams could be moved entirely independently of one another. Figure 7(b) shows how the problem with sets 4B and 3C was corrected using this increased freedom.
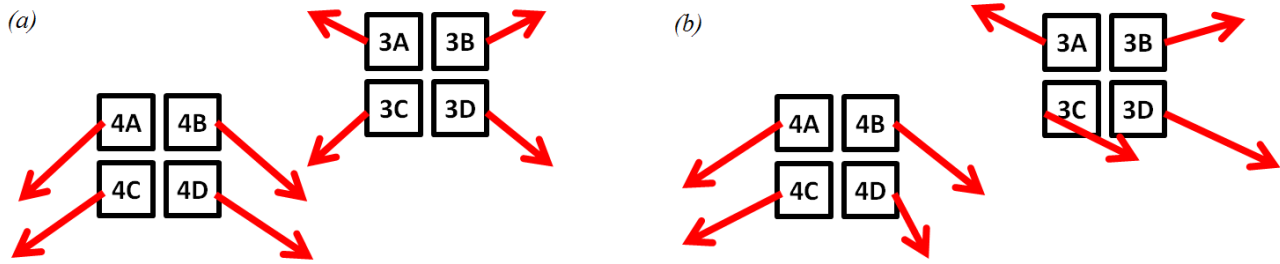
Figure 7: Approximation of beam pointings given to each beam in Rings 3 and 4. Beam sets are labeled. (a) In Tucker's design, beams were moved in pairs with the same vertical shift and opposite horizontal shifts. Note that beams 4B and 3C are shifted towards each other due to the nature of the shifting options, a phenomenon that decreases uniformity. (b) In the optimized design, each beam is given independent vertical and horizontal shifts.

The set of quads used in each ring could be changed. At the poles, it was possible to choose to use Ring 1 in both hemispheres, Ring 2 in both hemispheres, or Ring 1 in one hemisphere and Ring 2 in the other. At the equator, every other quad was taken in each of Rings 3 and 4. However, it was possible to choose which set of quads were taken, providing four different combinations of quad choices at the equator in each hemisphere.

3.2. Optimization Process and Optimized Designs

The goal of the optimization process was to develop a design, using 24 of the 48 of the quads on the NIF, that would result in as uniform an implosion as possible. A large number of 2-D hydrodynamic simulations were run using the code *SAGE* and then analyzed. These simulations used different variations of pointings, defocuses, and quad choices to determine the parameters for the optimum design.

Figure 8(a) shows the pulse that was put into the compression beams. The laser power increases to almost 90 terawatts, and the pulse ends just after 4 ns. Figure 8(b) is a ray trace plot for beam set 4A at 4 ns. The target has imploded from 900 microns to 465 microns. The critical surface can be seen in

11

this plot as the green contour line. Rays approach the target and deposit most of their energy at the critical surface as they refract away. The center of the beam shown in Figure 8(b) is aimed towards the equator of the target as is required for polar drive. 3-D ray tracing is used in the simulations.
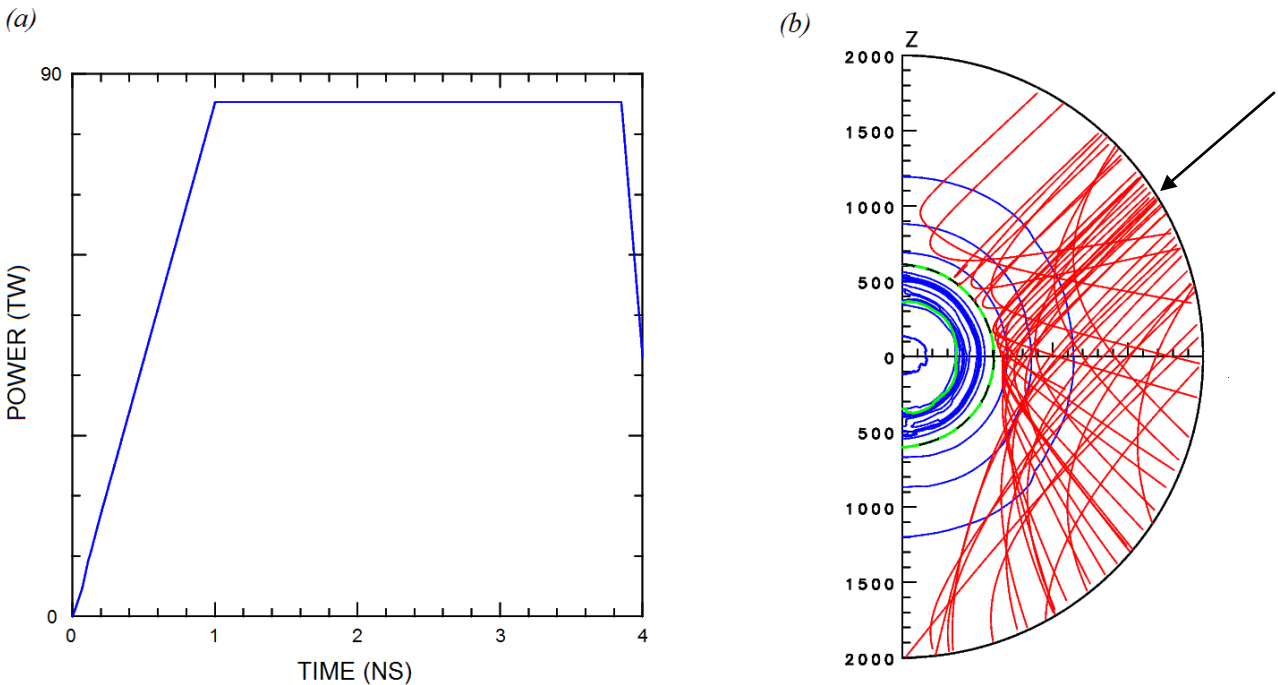

Figure 8: (a) Graph of power versus time of the compression pulse used in the NIF simulations. (b) Ray trace plot of a target after it has imploded from a radius of 900 microns to 465 microns. The critical surface is visible as the green ring. Beams refract away from the target close to the critical surface. The arrow indicates the direction of the laser beam.

Simulations were improved primarily through the use of sinusoidal projections of the target such as Figure 4 in Section 3 above. The effects of beam shifts and quad choice could be clearly seen on a projection depicting deviation in microns from the average center of mass over the target surface.

By adjusting the shifts of the beams and the quads used for the compression pulse, the optimum uniformity was reached. Energy deposition profiles for individual sets of beams, such as the one seen in Figure 9, were used to see where each beam deposits its energy. By comparing the individual energy deposition profile for each of the twenty four sets of beams to the center of mass profile of the target, it

was possible to see which beams were depositing their energy in areas of overcompression and which were depositing their energy in areas of undercompression. Each of the twenty four sets was then shifted simultaneously in the next simulation towards an area of undercompression to improve upon the uniformity of the design. This method of optimization does not follow a step by step progression attempting to improve each beam shift individually. This would have resulted in an optimal beam shift in relation to the position of the other beams, but as soon as the other beams were moved they might affect which areas are the least compressed, meaning that the former optimal position would no longer provide the best uniformity. Changing all the beam shifts simultaneously until no further improvements were made avoided this issue altogether. Once this point was reached, only one or a few of the beams would be moved at a time, sometimes by different amounts in several simulations so that the optimal beam shifts could be found.
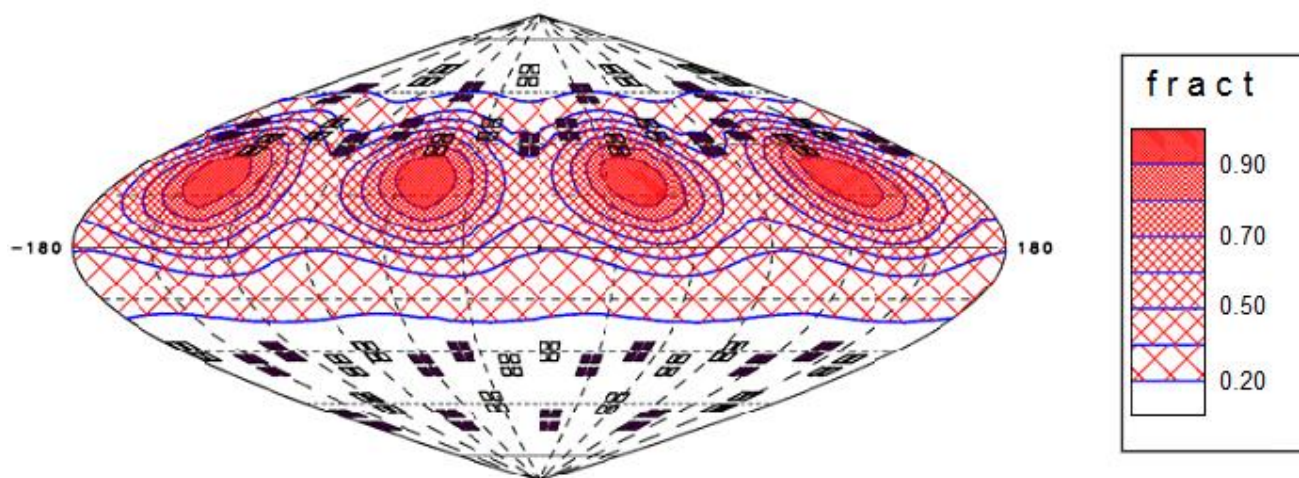

Figure 9: Energy deposition over the target surface by the beams in set 4A.

This method was pursued with several different choices of quads. Tucker's design had different patterns of quad choices in the top and bottom hemispheres. Both hemispheres in her design contained the same x and y shifts, but they were applied to different quad choices. This led to areas of more

13

significant overcompression in the bottom hemisphere and areas of more significant undercompression in the top hemisphere. Some simulations were run using different x and y pointings in the top and bottom hemispheres and the same quad choices in order to correct these issues. Others used the same patterns of quad choices in the top and bottom. The optimized design used the same quad choices as Tucker's design in the top hemisphere, but used the lowermost ring of beams in the bottom hemisphere, Ring 8 instead of Ring 7, in order to produce patterns in the top and bottom hemispheres that would overlap at the equator with a high uniformity.

The beam defocuses in Tucker's design provided a good level of uniformity without compromising the laser energy absorbed. Only minor changes to the beam defocuses were made.

Figure 10 shows the optimized design, which has an rms of 0.74%, or 3.5 microns, after the target has imploded to 456 microns, over a factor of two lower than the 1.81% rms of Tucker's design. This value is also well below the 1% rms thought to be required for ignition.[1] The parameters for the optimized design are listed in Table 1.
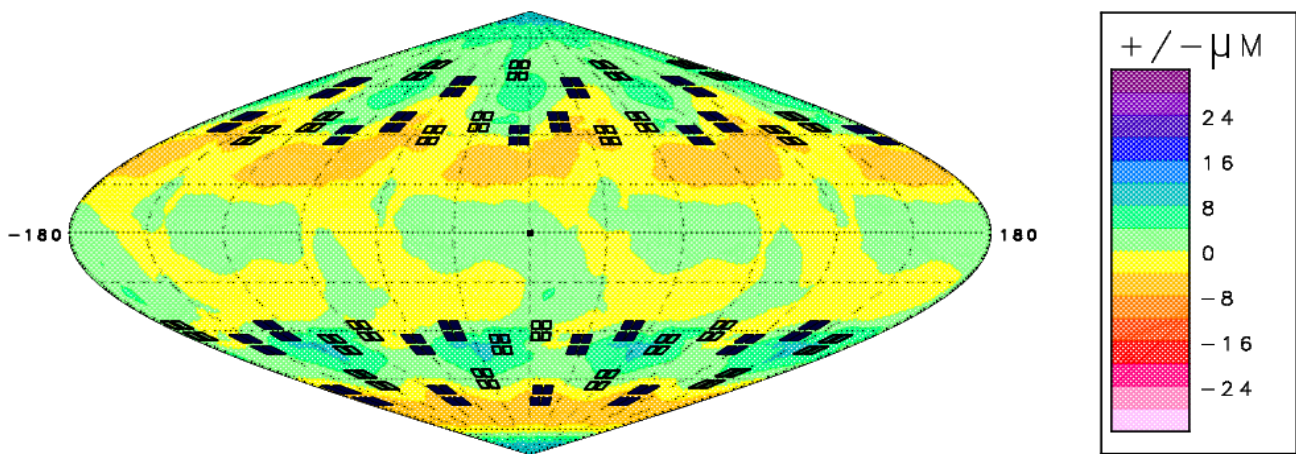

Figure 10: 3-D center of mass profile depicting non-uniformity over the target surface after 4 ns in the optimized design on the same scale as Figure 4. Yellow and orange areas represent lower than average center of mass radii, while green areas represent with higher than average center of mass radii. The non-uniformity in the center of mass has been reduced by a factor of two from Tucker's design, with an rms of 0.74%, or 3.5 microns, after the target has imploded past 435 microns.

This design has the advantage of being usable for the shock beam pointings due to the quad choices in the two hemispheres, namely the use of non-corresponding rings in each hemisphere: Ring 2 in the top hemisphere and Ring 8 in the bottom hemisphere. It is possible to map the parameters from the upper hemisphere for the compression pulse to the lower hemisphere for the shock pulse, and vice versa, and then to scale the pointings used for the compression pulse to the decreased size of the target after 4 ns. This should greatly simplify the development of the overall experimental design.

Set	θ	a, b (microns)	Defocus (cm)	Vertical Shift (microns)	Horizontal Shift (microns)	Number of beams used
1A	21.24	882, 631	–	–	–	0
1B	25.93	882, 631	–	–	–	0
2A	28.01	824, 590	2.9	36	-200	8
2B	32.70	824, 590	2.9	-24	300	8
3A	42.19	635, 367	2.6	182	-350	4
3B	42.19	635, 367	2.6	132	405	4
3C	46.89	635, 367	2.0	-318	270	4
3D	46.89	635, 367	2.0	-342	475	4
4A	47.68	593, 343	1.6	-397	-540	4
4B	47.68	593, 343	1.6	-487	415	4
4C	52.38	593, 343	1.4	-490	-545	4
4D	52.38	593, 343	1.4	-532	120	4

Table 1: Beam parameter specifications for the twelve beam sets in the upper hemisphere of the optimized design. Positive vertical shifts indicate shifts towards the poles, while negative values indicate shifts toward the equator. Positive horizontal shifts indicate rightward shifts, while negative values indicate leftward shifts. The values of a and b indicate the half-intensity focal spot radii of the phase plates currently installed on the NIF.

4. Experimental Designs for OMEGA

Before attempting shock ignition experiments on the NIF, experiments have been performed on OMEGA to investigate shock ignition on a smaller scale.[10] Preliminary experiments using forty beams for the compression pulse and twenty beams for the shock pulse were only partly successful due to non-uniform implosion of the target. To remedy this issue, beam pointing parameters were adjusted in order to increase the uniformity of energy deposition over the target surface. Optimization on OMEGA focused on compensating for the irregular beam arrangement. There was no ability to choose which beams would deliver the pulse due to the design of the laser system.

Figure 11 shows the shape of the laser pulse proposed for future experiments.[10] The lower power pulse is the compression pulse put into the forty beams. The higher power pulse which joins it at 2.6 ns is the shock pulse which is put into the twenty beams. The three pickets that come in the early part of the compression pulse launch shock waves that increase the compression of the target.
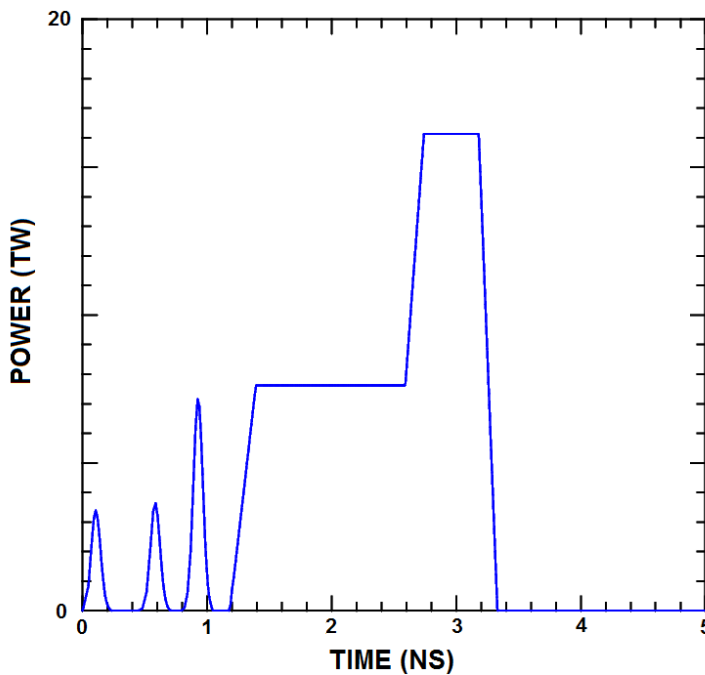

Figure 11: Graph of power versus time of the pulse used for OMEGA simulations. The compression pulse continues until 3.3 ns. The shock pulse turns on at 2.6 ns and ends at the same time as the compression pulse.

4.1. Optimized Design for the Compression Beams

The spacing of the forty compression beams leads to areas of high and low energy deposition. Figure 12 is an energy deposition profile calculated for beam pointing parameters used in preliminary experiments.[11] Shaded circles represent the beams delivering the compression pulse, and unshaded circles represent the beams that deliver the shock pulse later in the experiment. It is clear that there are areas of high and low energy deposition corresponding to areas where there are many compression beams and areas where there are few compression beams, respectively.
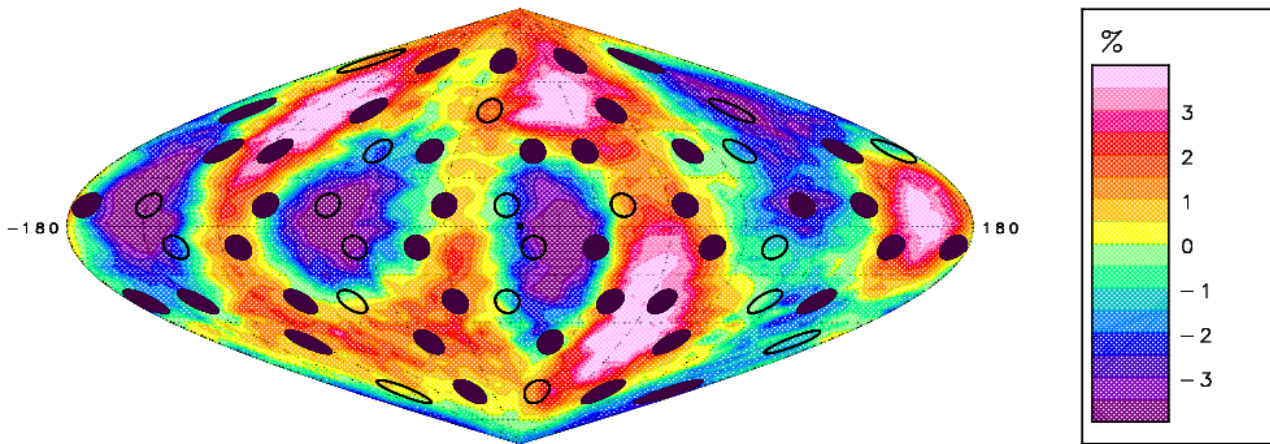

Figure 12: 3-D energy deposition profile showing non-uniformity on the target surface integrated up to 2.5 ns using Gotchev's beam pointings [Ref. 11]. The non-uniformity of the target is 2.11% averaged over the surface of the target. Yellow and pink areas indicate above average energy deposition, while green and purple areas indicate below average energy deposition.

The only parameters available to improve uniformity for the compression beams were beam shifts. These were optimized in much the same way as they were for the NIF design. Adjusting these shifts for OMEGA presented more of a challenge because each of the forty beams had to be shifted individually, rather than in symmetrical rings around the surface of the target. There were eighty different parameters to optimize, two per laser beam. The optimized design is shown in Figure 13. It has a uniformity of 1.19% rms, almost a factor of two better than the previous design.
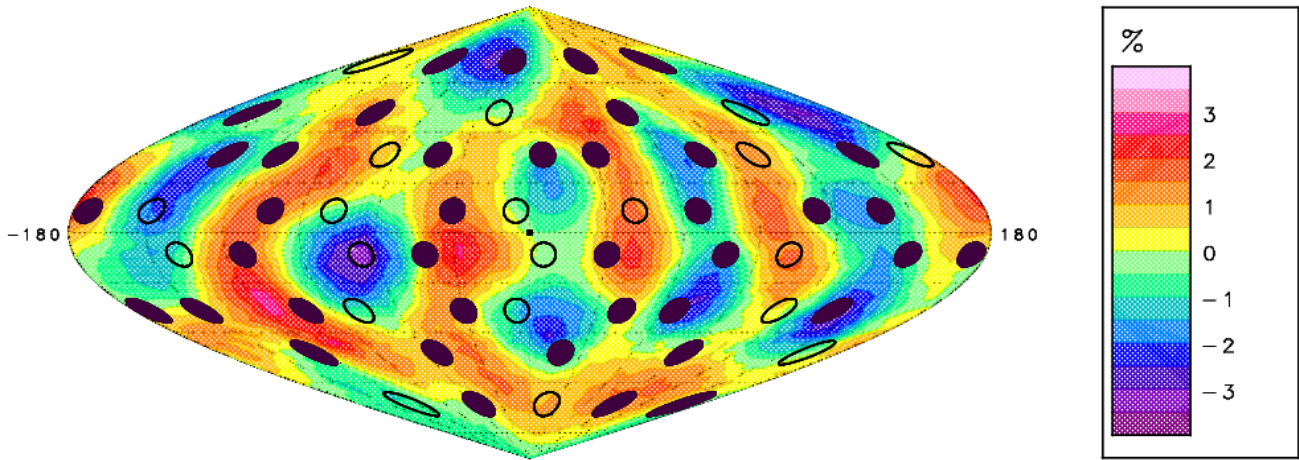
Figure 13: 3-D energy deposition profile showing non-uniformity on the target surface after 2.5 ns in the optimized design for the forty compression beams on OMEGA. This profile is on the same scale as Figure 12.

4.2. Optimized Design for the Shock Beams

The previous design[12] used for the shock beams assumed that pointing each of the twenty beams directly at one of the vertices of a dodecahedron on the initial target surface would be optimum. A simulation run on *SAGE* [Figure 14] showed that this design produced a non-uniformity of 6.7% rms.

The method for optimizing uniformity used for the shock beams was the same as the method used for the forty compression beams, though the smaller number of beams available made optimization more difficult. In areas with a high concentration of beams, such as the group of three beams seen in the center of the target in Figure 14, it was extremely difficult to lower the energy deposition. Similarly, it was extremely difficult to increase energy deposition in areas without many shock pulse beams in the vicinity.

These difficulties achieving uniform energy deposition can be explained by the way energy is deposited as beams travel past the target. Beams do not deposit all their energy in the one spot on the target at which they are pointed; instead they travel through plasma around the target and then refract
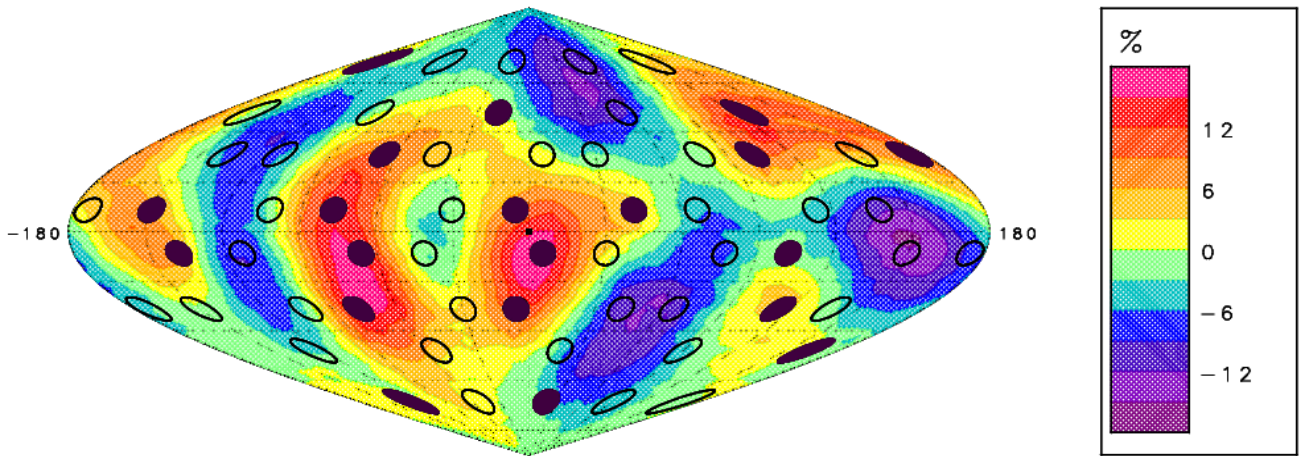
Figure 14: 3-D energy deposition profile showing non-uniformity on the target surface after 4 ns in the previous design for the 20 shock beams on OMEGA. This design has a non-uniformity of 6.7% rms averaged over the target surface. Yellow and pink areas indicate above average energy deposition, while green and purple areas indicate below average energy deposition.

away once they reach the critical surface as shown in Figure 8, with energy being deposited all the while. Beams are also nearly as large as the target, so even when they are shifted to provide greater energy to another part of the target, they still hit the same spot they would if they were pointed at the center of the target. A significant amount of energy is still deposited at that location because the rays at this point on the target are at normal incidence, allowing them to approach much closer to the critical surface and deposit more energy nearer to the center of the target. This makes it impossible to achieve anything but a higher than average energy deposition in these areas without repointing the beams so far that energy absorption by the target greatly decreases.

However, the optimized design did improve significantly upon the initial design. The optimized design can be seen in Figure 15. It has a non-uniformity of 3.9% rms, a significant improvement over the 6.7% rms of the previous design. It is also believed that the uniformity of the shock beams is less significant than for the compression beams since by the time the shock beams turn on, there will be a large plasma surrounding the target. Thermal conduction through the plasma will reduce non-uniformity caused by the shock beams.
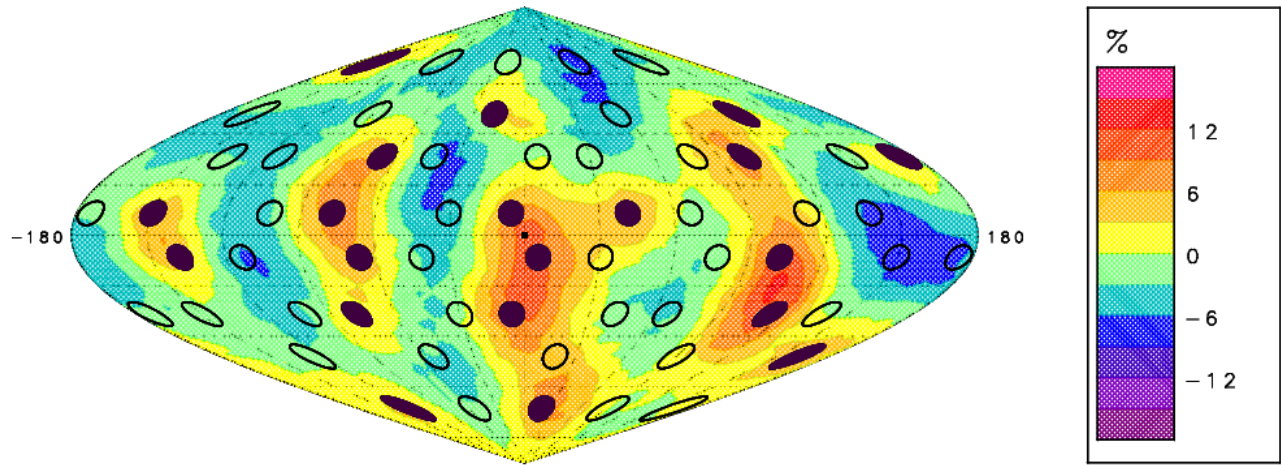
Figure 15: 3-D energy deposition profile showing non-uniformity over the target surface after 4 ns in the optimized design for the 20 shock beams on OMEGA on the same scale as Figure 14. This design has a non-uniformity of 3.9% rms.

5. Conclusion

Designs have been developed for shock ignition experiments on the NIF and OMEGA to provide optimum implosion uniformities. These were designed using 2-D hydrodynamic simulations with 3-D ray tracing. The experiment to be performed on the NIF utilizes polar drive to overcome the indirect drive setup of the laser facility, and the experimental design involves adjusting beam defocuses, quad choices, and beam shifts. The optimized design for the compression beams results in non-uniformity of 0.74% rms, which is more than a two-fold improvement over the previous non-uniformity of 1.81% rms. Due to the choice of configuration of the quads used for the compression pulse, the design can also be used for the shock beams by making some minor adjustments.

For OMEGA, beam shifts are required to account for the irregular arrangement of the forty compression beams and the twenty shock beams to be used in future experiments. The optimized design for the compression beams has a non-uniformity of 1.2% rms, nearly twice as small as the 2.1% rms non-uniformity in the previous design. The optimized design for the shock beams has a non-

uniformity of 3.9% rms, an improvement on the 6.7% rms non-uniformity in the previous design.

Using these designs, it will be possible to test the feasibility of shock ignition in experiments on OMEGA and the NIF.

6. Acknowledgments

References

[1] J. Nuckolls et al., "Laser Compression of Matter to Super-High Densities: Thermonuclear (CTR) Applications," Nature **239**, 139 (1972).

[2] R. Betti et al., "Shock Ignition of Thermonuclear Fuel with High Areal Density," Phys. Rev. Lett. **98** (15), 155001 (2007).

[3] R. S. Craxton et al., "Polar Direct Drive: Proof-of-Principle Experiments on OMEGA and Prospects for Ignition on the National Ignition Facility," Phys. Plasmas **12**, 056304 (2005).

[4] J. A. Marozas et al., "Polar-Direct-Drive Simulations and Experiments," Phys. Plasmas **13**, 056311 (2006).

[5] S. Skupsky et al., "Polar Direct Drive on the National Ignition Facility," Phys. Plasma **11**, 2763 (2004).

[6] R. S. Craxton and D. W. Jacobs-Perkins, "The Saturn Target for Polar Direct Drive on the National Ignition Facility," Phys. Rev. Lett. **94**, 095002 (2005).

[7] Laura A. Tucker, "A Design for a Shock Ignition Experiment on the NIF Including 3-D Effects," Laboratory for Laser Energetics High School Summer Research Program (2010).

[8] R. S. Craxton and R. C. McCrory, "Hydrodynamics of Thermal Self-Focusing in Laser Plasmas," J. Appl. Phys. **56**, 108 (1984).

[9] A. M. Cok et al, "Polar-drive designs for optimizing neutron yields on the National Ignition Facility," Phys. Plasmas **15**, 082705 (2008).

[10] K. Anderson, unpublished.

[11] O. Gotchev, unpublished.

[12] W. Theobald, unpublished.